NASA TECHNICAL NOTE

NASA TN D-4567

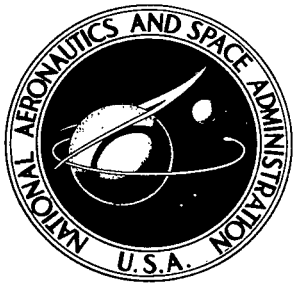


NASA TN D-4567



# YIELDING AND FRACTURE IN TUNGSTEN AND TUNGSTEN-RHENIUM ALLOYS

*by Peter L. Raffo*

*Lewis Research Center*
*Cleveland, Ohio*

NATIONAL AERONAUTICS AND SPACE ADMINISTRATION • WASHINGTON, D. C. • MAY 1968

# YIELDING AND FRACTURE IN TUNGSTEN AND TUNGSTEN-RHENIUM ALLOYS

By Peter L. Raffo

Lewis Research Center
Cleveland, Ohio

NATIONAL AERONAUTICS AND SPACE ADMINISTRATION

For sale by the Clearinghouse for Federal Scientific and Technical Information
Springfield, Virginia 22151 – CFSTI price $3.00

## ABSTRACT

A study was made of the mechanical properties of vacuum arc-melted tungsten and tungsten-rhenium alloys in the temperature range $77^{o}$ to $810^{o}$ K in order to elucidate the mechanism by which rhenium additions lower the ductile-brittle transition temperature of tungsten. The temperature and strain-rate dependency of the yield stress of tungsten is reduced by alloying with rhenium. This is shown to be because of a reduction in the Peierls stress. The reduction in the transition temperature is attributed to the reduced Peierls stress through its effect on the mobility and rate of multiplication of dislocations.

# YIELDING AND FRACTURE IN TUNGSTEN AND TUNGSTEN-RHENIUM ALLOYS

by Peter L. Raffo

Lewis Research Center

## SUMMARY

A study was made of the mechanical properties of vacuum arc-melted tungsten and tungsten-rhenium alloys in the temperature range $77^{\circ}$ to $810^{\circ}$ K. The ductile-brittle transition temperature of the unalloyed recrystallized tungsten prepared for this study was $490^{\circ}$ K and was reduced to $430^{\circ}$ and $350^{\circ}$ K by additions of 2 and 25 percent rhenium (Re), respectively. The temperature and strain rate dependence of the yield stress of tungsten is decreased by alloying with rhenium. The work-hardening rate of 1-percent plastic strain for unalloyed tungsten (W) increases rapidly with decreasing temperature, although it is relatively independent of temperature in the W-Re alloys. In unalloyed tungsten and dilute W-Re alloys, fracture was mainly by cleavage. In these materials, fracture is controlled by crack initiation; in the W-25-percent-Re alloy, failure is controlled by crack propagation. The observations suggest that yielding of unalloyed tungsten is controlled by the nucleation of kink pairs over the Peierls barrier. Alloying with rhenium reduces the Peierls stress. The yielding of a W-25-percent-Re alloy is controlled by a similar mechanism at low temperatures; at higher temperatures, an apparent decrease in the s tacking-fault energy alters the yielding mechanism to one in which it is controlled by the recombination of dissociated screw dislocations. The reduction in the transition temperature in W-Re alloys is thought to be caused by the stress relaxation effect of an increased plastic-strain rate at the tip of a crack as a result of increased dislocation mobilities and multiplication rates.

## INTRODUCTION

The applications of tungsten and its alloys have been limited to a great extent by their brittleness at ambient temperatures. Typical ductile-brittle transition temperatures for arc-melted tungsten sheet range from approximately $475^{\circ}$ to $525^{\circ}$ K and $560^{\circ}$ to $645^{\circ}$ K for wrought and recrystallized sheet, respectively (ref. 1). High ductile-brittle transition temperatures are not peculiar to tungsten; they also characterize the other group VI metals, molybdenum and chromium (ref. 2).

Various theories have been advanced to explain the brittleness of these metals, with varying degrees of success. The fact that the transition temperature is sensitive to the presence of interstitial impurities has received the most attention and is supported by the fact that zone purification of molybdenum and tungsten has resulted in significant decreases in the transition temperature (refs. 3 and 4). The major effect of interstitials appears to be related to their interaction with grain boundaries either in solid solution or as a precipitate (ref. 5), since single crystals of the group VI metals are ductile at temperatures well below ambient. Other theories advanced to explain the extreme brittleness are based on the intrinsic properties of dislocations in tungsten, molybdenum, and chromium in that the low dislocation mobility in these metals does not allow gross plastic flow to occur in front of propagating cracks which would tend to blunt them (ref. 5).

A very effective way to lower the ductile-brittle transition temperature of tungsten is by alloying with rhenium (ref. 7). Additions of rhenium as low as 1 percent (all compositions in atomic percent) are capable of producing a noticeable decrease in the transition temperature; however, much larger decreases in the transition temperature occur in more concentrated alloys, particularly those near the solvus line. A reproduction of the tungsten-rhenium (W-Re) phase diagram is shown in figure 1 (ref. 6). These effects have also been observed in molybdenum (ref. 8) and chromium (ref. 9) alloyed with rhenium. In addition, other chromium base systems, such as chromium-ruthenium, chromium-iron, and chromium-cobalt, also show improved ductility near the solvus line (ref. 10).

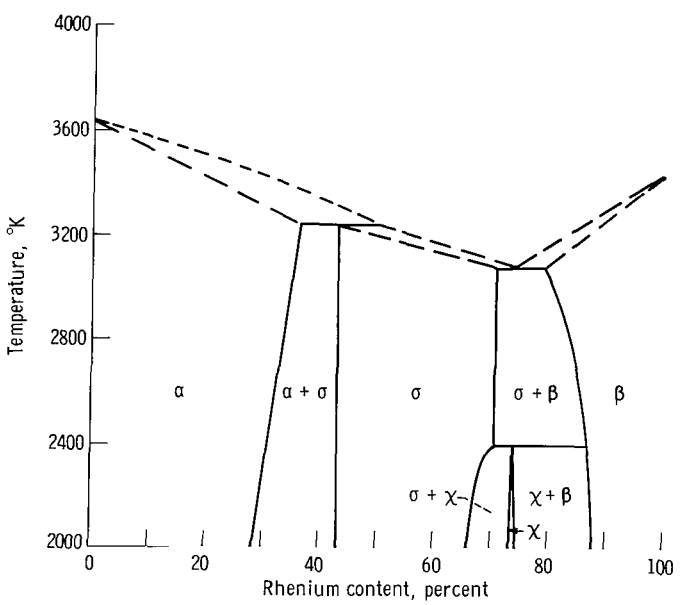


Figure 1. - Tungsten-rhenium phase diagram (ref. 6).

The present investigation was initiated in order to provide some basic mechanical property data on the temperature and strain-rate sensitivity of the yield stress in polycrystalline W and W-Re alloys. It was anticipated that such information would lead to a better understanding of the brittle fracture process in these materials because it is thought that the relative ease of dislocation motion controls the ease of crack propagation. Both dilute alloys (1- to 7-percent Re) and an alloy whose composition (25-percent Re) is near the solvus line were studied.

## SYMBOLS

| | |
|---|---|
| $b$ | Burger's vector |
| $c$ | constant |
| $E_c$ | line tension at top of Peierls barrier |
| $E_o$ | equilibrium line tension |
| $H$ | activation energy |
| $H_o$ | thermal energy needed to bypass obstacle in absence of stress |
| $k$ | Boltzmann's constant, $1.38\times10^{-23}$ (J)($^{o}$K) |
| $T$ | temperature |
| $T_d$ | ductile-brittle transition temperature |
| $T_r$ | reference temperature |
| $T_0$ | temperature where $\sigma^* = 0$ |
| $2U_K$ | energy to form pair of kinks |
| $V^*$ | activation volume |
| $z$ | constant |
| $\gamma'$ | stacking fault energy on {112} planes |
| $\dot{\epsilon}$ | strain rate |
| $\dot{\epsilon}_o$ | frequency factor |
| $\lambda$ | strain-rate sensitivity of yield stress |
| $\mu$ | shear modulus |
| $\sigma$ | tensile strength |

$\sigma^*$ effective stress

$\sigma_F$ brittle fracture stress

$\sigma_y$ yield stress

$\sigma_{yc}$ yield stress in compression

$\sigma_{yt}$ yield stress in tension

$(\Delta\sigma)_T$ change in stress after tenfold change in strain rate

$\sigma_\mu$ athermal component of yield stress

$\tau$ shear stress; for polycrystalline materials, $\tau = 1/2\ \sigma$

$\tau^*$ effective shear yield stress

$\tau_p$ Peierls stress

$\tau_0^*$ value of $\tau^*$ at absolute zero

## EXPERIMENTAL PROCEDURES

The unalloyed tungsten and tungsten-rhenium alloys used in this program are listed in table I together with carbon and oxygen analyses sampled from the swaged rod. In addition, the grain sizes obtained on the rod after a 1-hour anneal at 2255° K are listed. Fabrication techniques used for the alloys have been documented previously (ref. 7).

TABLE I. - ANALYSIS OF MATERIALS

| Alloy | Analyzed rhenium content, at. % | Interstitial analyses, ppm | | Average grain diameter after 1-hr anneal at 2255° K, cm |
|---|---|---|---|---|
| | | Oxygen | Carbon | |
| Unalloyed tungsten | 0 | 2 | 4 | $3.96\times10^{-3}$ |
| W-1-percent Re | 1.0 | 3 | 3 | 5.29 |
| W-2-percent Re | 2.0 | 2 | 4 | 6.39 |
| W-7-percent Re | 6.8 | 12 | 3 | 3.68 |
| W-25-percent Re | 24.8 | 4 | 6 | 6.08 |

Briefly, the procedure consisted of initially arc or electron-beam melting of sintered electrodes in vacuum, followed by hot extrusion to bar stock. The extruded bar was then swaged to either 0.25 inch (0.64 cm) or 0.33 inch (0.84 cm). Buttonhead tensile specimens of the type previously described in reference 11 were ground from the swaged rod with a 0.14- or 0.16-inch (0.37- or 0.42-cm) gage diameter and a 1-inch (2.54-cm) gage length. The specimens were recrystallized in vacuum for 1 hour at 2255° K. Prior to testing, the specimens were electropolished in a 2-percent sodium hydroxide solution at 12 to 15 volts.

Tensile tests were performed at a strain rate of approximately $8.3\times10^{-4}$ $sec^{-1}$ using a split-grip arrangement. Above room temperature, the specimens were heated in air in a quartz-tube radiation furnace. Below 298° K various temperatures were obtained by blowing cold nitrogen gas onto the specimen in an apparatus similar to that described by Wessel (ref. 12). The temperature was measured by a copper-constantan thermocouple. Compression tests were performed at approximately the same strain rate, although there was some scatter (~10 percent) due to minor differences in the initial gage length of the specimen. The compression specimens were nominally 0.25- or 0.13-inch (0.66- or 0.34-cm) diameter and 0.6- and 0.3-inch (1.52- or 0.79-cm) long. The specimens were tested in a modified fixture of the type employed by Alers, Armstrong, and Bechtold (ref. 13). The ends of the specimen were lubricated with aluminum foil to minimize the buildup of secondary tensile stresses due to friction. Similar heating and cooling techniques were employed for both the compression tests and the tensile tests; however, a few compression tests were performed at liquid-nitrogen temperatures (77° K) by immersing the entire fixture in a liquid-nitrogen bath.

The tensile tests were conducted to failure, while the compression specimens were strained to approximately 5 percent. In several tests, the strain rate was cycled by a factor of 10 during the course of the test to determine the strain-rate sensitivity. Metallographic studies were conducted on longitudinally sectioned samples that were electropolished in a 2-percent sodium hydroxide solution at 12 to 15 volts. Etching was performed in boiling 3-percent hydrogen peroxide.

# RESULTS

## Yielding and Fracture

Unalloyed tungsten. - The mechanical property data for unalloyed tungsten are listed in table II. Figure 2 illustrates the effect of temperature on the ductility of arc-melted tungsten annealed at 2255° K for 1 hour. The data fell within the narrow scatter band (~30° K) which had been obtained previously for different lots of recrystallized arc-melted tungsten (ref. 11).

TABLE II. - MECHANICAL PROPERTIES OF UNALLOYED ARC-MELTED TUNGSTEN

Annealed at 2255° K for 1 hr.

| Temperature, °K | Yield stress in tension, $\sigma_{yt}$ | | Fracture stress in tension, $\sigma_F$ | | Ultimate tensile stress in tension | | Reduction in area, percent | Elongation, percent | Yield stress in compression | |
|---|---|---|---|---|---|---|---|---|---|---|
| | ksi | $MN/m^2$ | ksi | $MN/m^2$ | ksi | $MN/m^2$ | | | ksi | $MN/m^2$ |
| 77 | ----- | --- | ---- | --- | --- | --- | - | ---- | 195.80 | 1350 |
| 200 | ----- | --- | ---- | --- | --- | --- | - | ---- | 130.30 | 898 |
| 228 | ----- | --- | ---- | --- | --- | --- | - | ---- | 119.10 | 821 |
| 298 | ----- | --- | 80.6 | 556 | --- | --- | 0 | 0 | 86.10 | 594 |
| 366 | ----- | --- | 59.6 | 411 | --- | --- | 0 | 0 | 62.70 | 432 |
| 477 | ----- | --- | 45.8 | 316 | --- | --- | 0 | 0 | 37.7 | 260 |
| 545 | 30.50 | 210 | ---- | --- | --- | --- | - | ---- | ------ | ---- |
| 533 | 27.80 | 192 | ---- | --- | --- | --- | - | 16.4 | ------ | ---- |
| 589 | 29.80 | 205 | ---- | --- | 54.2 | 374 | - | 67.0 | ------ | ---- |
| 592 | 21.8 | 150 | ---- | --- | 68.3 | 471 | - | 77.0 | ------ | ---- |
| 680 | 13.4 | 92 | ---- | --- | 61.4 | 423 | - | 76.0 | ------ | ---- |

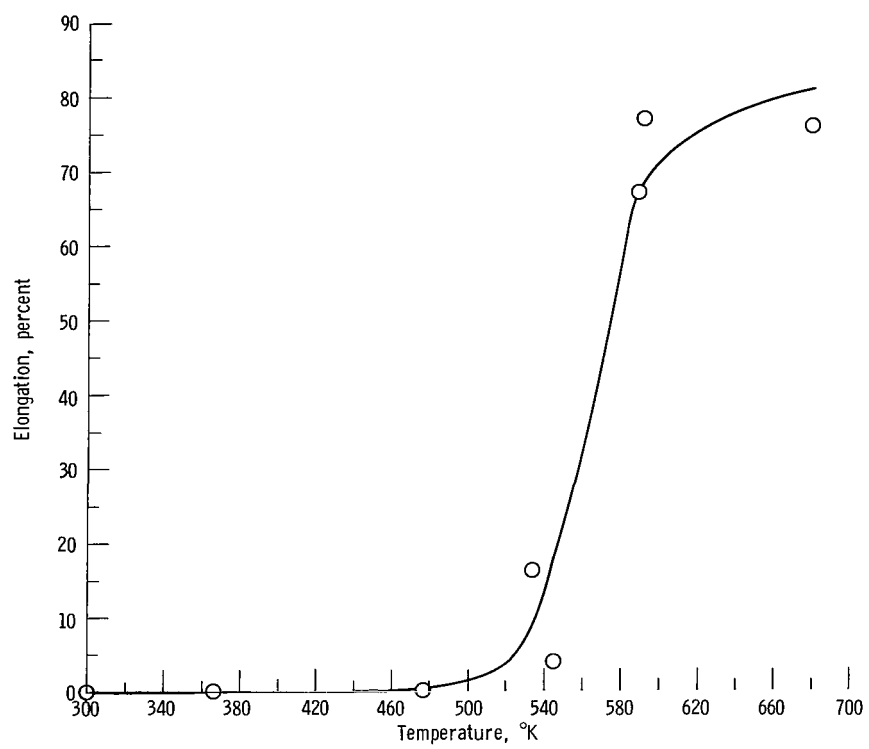


Figure 2. - Variation of ductility with temperature for arc-melted tungsten.

Strength values obtained for arc-melted tungsten are shown in figure 3. The plot contains the yield stresses in tension $\sigma_{yt}$ and compression $\sigma_{yc}$ in addition to the brittle fracture stress in tension $\sigma_F$. Two features are immediately evident: (1) $\sigma_{yt}$, $\sigma_{yc}$, and $\sigma_F$ fall on a continuous curve over the entire temperature range ($77^o$ to $680^o$ K), and (2) the yield stress increases rapidly with decreasing temperature, in common with other body centered cubic (BCC) metals. These observations indicate that brittle fracture in unalloyed tungsten occurs at stress levels consistent with the level for macroscopic yielding. This result has been well documented in the literature for various BCC metals including steels (ref. 14), molybdenum (ref. 15), and tungsten (ref. 16).

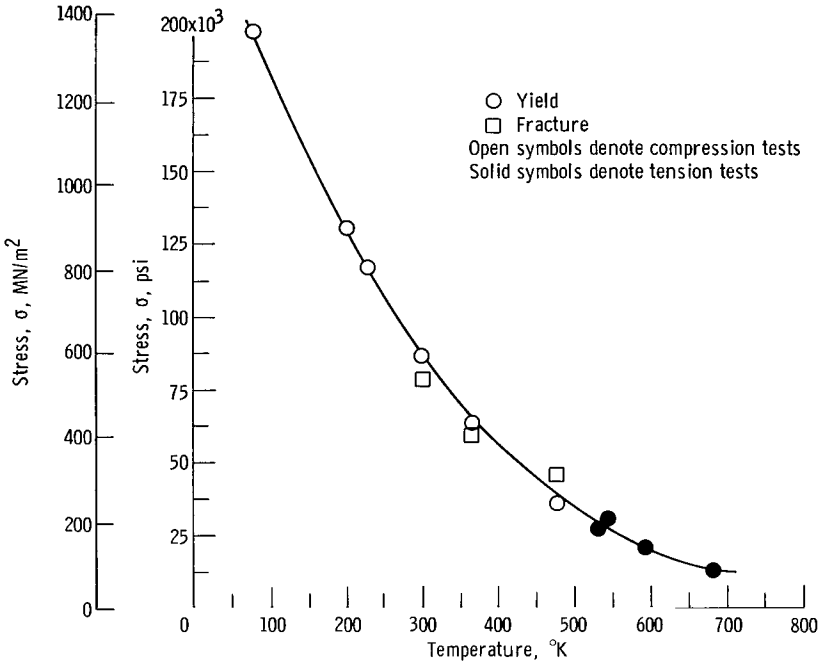


Figure 3. - Effect of temperature on yield and fracture stresses of arc-melted tungsten.

Tungsten-Rhenium alloys. - Mechanical property data for the recrystallized W-Re alloys are given in table III and figures 4 to 7. Figure 4 illustrates the variation of the tensile ductility with temperature for four W-Re alloys compared with the previously described data for unalloyed tungsten. Above approximately $600^o$ K, the ductility decreased with increasing rhenium content and the slope of the ductility-temperature curves also decreased. No sharp change in ductility was noted for the W-25-percent Re alloy over the entire temperature range shown. For convenience, a ductile-to-brittle transition temperature $T_d$ will be defined as the temperature for 5-percent elongation (see

TABLE III. - MECHANICAL PROPERTIES OF ARC-MELTED TUNGSTEN-RHENIUM ALLOYS

[Annealed at 2255° K for 1 hr.]

| Temperature, °K | Yield stress in tension, $\sigma_{yt}$ | | Fracture stress in tension, $\sigma_F$ | | Ultimate tensile stress in tension | | Reduction in area, percent | Elongation, percent | Yield stress in compression | |
|---|---|---|---|---|---|---|---|---|---|---|
| | ksi | $MN/m^2$ | ksi | $MN/m^2$ | ksi | $MN/m^2$ | | | ksi | $MN/m^2$ |
| W-1-percent Re | | | | | | | | | | |
| 77 | ---- | --- | ---- | --- | ---- | --- | ---- | -- | 190.5 | 1313 |
| 298 | ---- | --- | ---- | --- | ---- | --- | ---- | -- | 107.7 | 743 |
| 450 | ---- | --- | ---- | --- | ---- | --- | ---- | -- | 55.3 | 381 |
| 477 | ---- | --- | 61.9 | 427 | ---- | --- | 0 | 0 | ----- | ---- |
| 533 | ---- | --- | 51.2 | 353 | ---- | --- | 0 | 0 | ----- | ---- |
| 560 | 27.3 | 188 | ---- | --- | 66.8 | 461 | 58 | 43 | ----- | ---- |
| 589 | 23.2 | 160 | ---- | --- | 64.2 | 443 | 52 | 51 | ----- | ---- |
| 644 | 16.7 | 115 | ---- | --- | 60.1 | 414 | 50 | 53 | ----- | ---- |
| 700 | 13.0 | 90 | ---- | --- | 54.6 | 376 | 46 | 76 | ----- | ---- |
| W-2-percent Re | | | | | | | | | | |
| 77 | ---- | --- | ---- | --- | ---- | --- | ---- | -- | 15.1 | 1207 |
| 298 | ---- | --- | ---- | --- | ---- | --- | ---- | -- | 90.0 | 621 |
| 477 | 42.6 | 294 | ---- | --- | 67.8 | 467 | 9 | 12 | ---- | ---- |
| 533 | 33.3 | 230 | ---- | --- | 68.9 | 475 | 14 | 22 | ---- | ---- |
| 589 | 30.4 | 210 | ---- | --- | 66.6 | 459 | 52 | 45 | ---- | ---- |
| 700 | 24.2 | 167 | ---- | --- | 59.3 | 409 | 47 | 46 | ---- | ---- |
| W-7-percent Re | | | | | | | | | | |
| 77 | ---- | --- | ---- | --- | ---- | --- | ---- | -- | 133.8 | 923 |
| 200 | ---- | --- | ---- | --- | ---- | --- | ---- | -- | 125.6 | 866 |
| 298 | ---- | --- | 99.0 | 683 | ---- | --- | 0 | 0 | 99.0 | 683 |
| 366 | ---- | --- | ---- | --- | ---- | --- | ---- | -- | 79.3 | 547 |
| 422 | 70.2 | 484 | ---- | --- | ---- | --- | 1.2 | 1 | ----- | ---- |
| 477 | 62.7 | 432 | ---- | --- | 96.5 | 665 | 14 | 9 | 62.2 | 429 |
| 589 | 57.5 | 396 | ---- | --- | 88.7 | 612 | 28 | 20 | 53.0 | 365 |
| 700 | 50.3 | 347 | ---- | --- | 79.7 | 550 | 32 | 30 | ----- | ---- |
| W-25-percent Re | | | | | | | | | | |
| 77 | ----- | --- | --- | --- | ----- | --- | ---- | -- | 151.3 | 1043 |
| 200 | ----- | --- | --- | --- | ----- | --- | ---- | -- | 117.3 | 809 |
| 298 | 105.7 | 729 | --- | --- | ----- | --- | 2 | 4 | ----- | ---- |
| 366 | 98.5 | 679 | --- | --- | ----- | --- | 5.5 | 6 | ----- | ---- |
| 477 | 96.7 | 667 | --- | --- | ----- | --- | 10 | 9 | ----- | ---- |
| 589 | 94.2 | 649 | --- | --- | 133.9 | 923 | 28 | 17 | ----- | ---- |
| 700 | 86.6 | 597 | --- | --- | 114.8 | 792 | 43 | 20 | ----- | ---- |
| 810 | 82.7 | 570 | --- | --- | 111.8 | 771 | 75 | 30 | ----- | ---- |

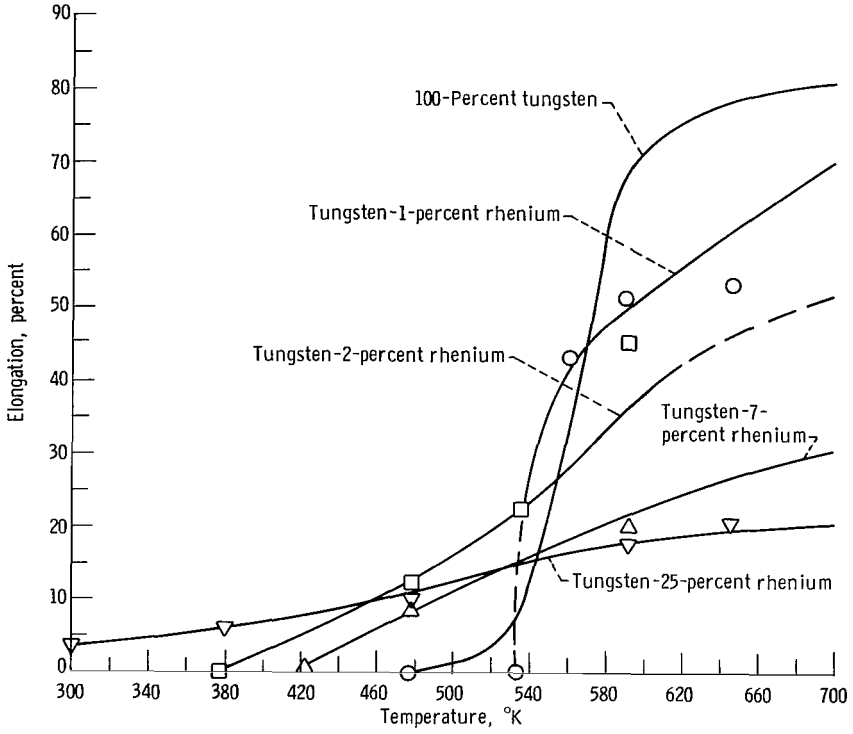


Figure 4. - Effect of rhenium on ductility of arc-melted tungsten.

TABLE IV. - TRANSITION TEMPERATURES

FOR ARC-MELTED TUNGSTEN AND

TUNGSTEN RHENIUM ALLOYS

| Rhenium content, at. % | Transition temperature, $^{o}K$ |
|---|---|
| 0 | 530 |
| 1.0 | 530 |
| 2.0 | 430 |
| 7.0 | 450 |
| 25.0 | 350 |

table IV). Additions of 2- and 7-percent Re lowered $T_d$ from 530° K for unalloyed tungsten to 430° and 450° K, respectively. An addition of 1-percent Re had no effect on $T_d$. The values of $T_d$ for W-25-percent Re is considerably lower, approximately 350° K. These results are in general agreement with those found previously by Klopp, et al. (ref. 7); however, in that work, a minimum in the transition temperature was found at 2- to 5-percent Re, but the fewer compositions tested here did not allow a confirmation of this minimum.

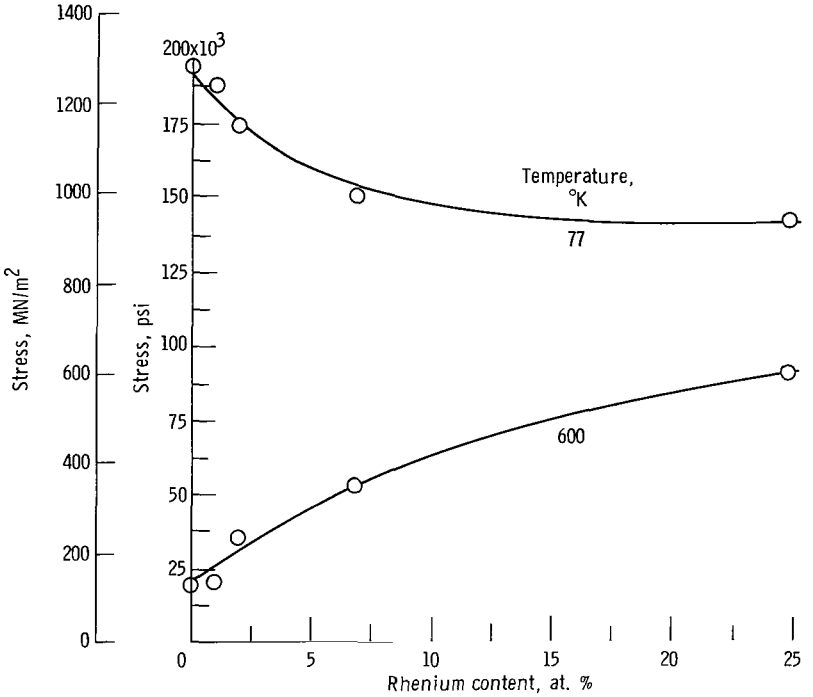


Figure 5. - Effect of composition on 77° and 600° K yield stresses.

The composition dependence of the yield stress at 77° and 600° K is given in figure 5. The yield stress increased continuously with concentration at 600° K. This is a normal solid solution hardening effect. But at 77° K the yield stress decreased with increasing rhenium content. This behavior, (which may be termed "solution softening") is commonly observed in BCC alloys at low temperatures (refs. 17 to 19). However, the W-Re alloys are unique in that alloy softening appears to be continuous with increasing solute content. Other alloy systems such as tantalum-rhenium and tantalum-molybdenum (ref. 17), iron-chromium (ref. 18) and iron-molybdenum (ref. 19) show a minimum at low concentrations after which the yield stress increases again.

The temperature dependence of $\sigma_y$ and $\sigma_F$ for W-Re alloys is shown in figure 6.

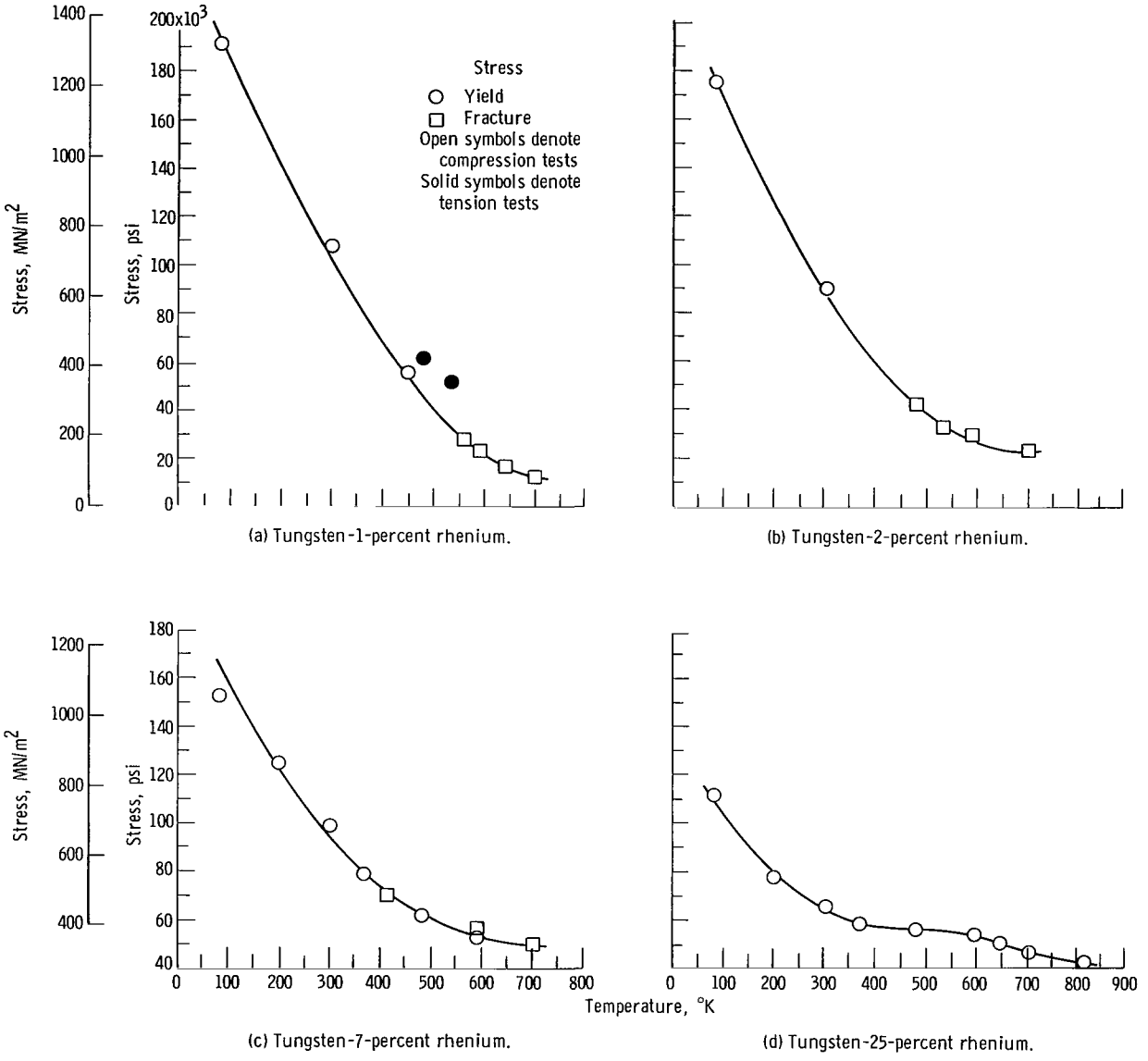


(a) Tungsten-1-percent rhenium.

(b) Tungsten-2-percent rhenium.

(c) Tungsten-7-percent rhenium.

(d) Tungsten-25-percent rhenium.

Figure 6. - Temperature dependence of yield and brittle fracture stresses for tungsten-rhenium alloys.

As in unalloyed tungsten, $\sigma_F$ fell close to the yield-stress temperature curve. The shape of the curves is similar to that for unalloyed tungsten, except for a broad plateau in the W-25-percent-Re data at 400° to 500° K. The differences between the alloys are better shown in figure 7 where the curves from figure 6 are replotted on one set of coordinates. The temperature ranges where alloy softening and hardening occur are clearly shown here.

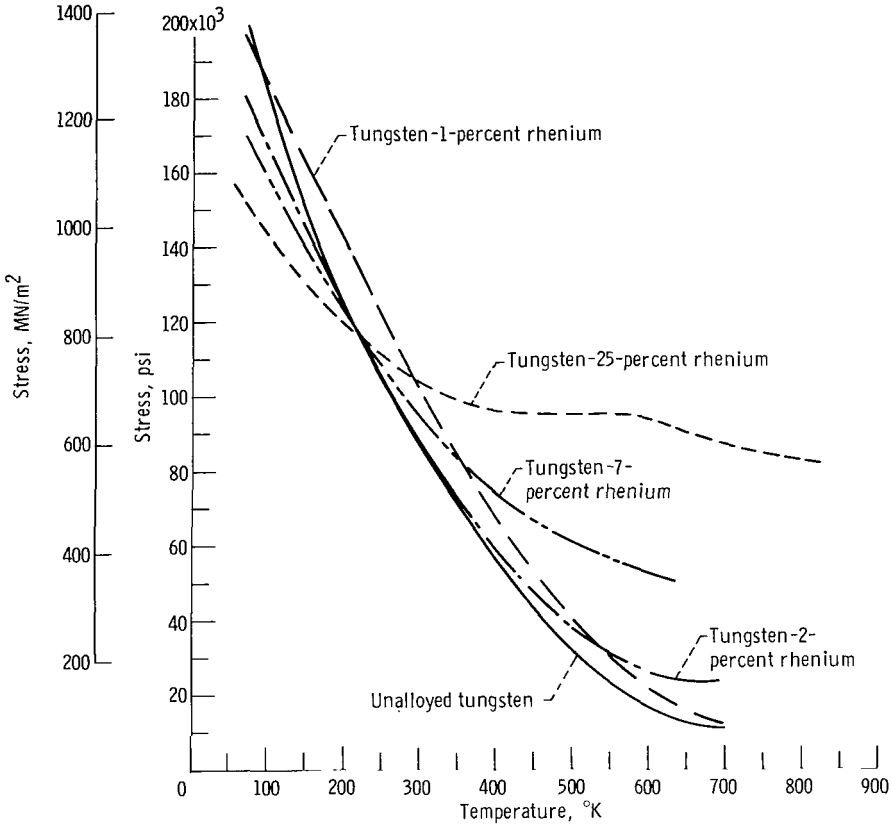


Figure 7. - Influence of temperature on yield stress of tungsten and tungsten-rhenium alloys.

Twinning in tungsten-25-percent-rhenium. - The 25-percent-Re alloy deformed partially by twinning at temperatures up to 800° K. An indication of the degree of twinning is illustrated in figure 8 where the lineal twin density after deformation to fracture is plotted against temperature. The twin density was uniform throughout the fractured gage section even though some of the specimens had necked slightly. This suggests that all the twins are nucleated early in the stress-strain cycle, and that they fill the entire gage section. This has been demonstrated in molybdenum-rhenium alloys by Underwood

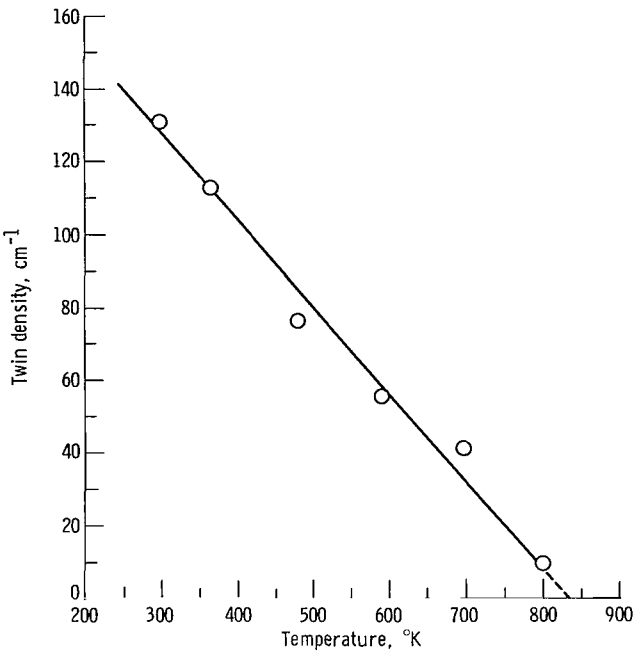


Figure 8. - Variation of twin density in fractured tungsten-25-percent rhenium with temperature.

and Coons (ref. 20), who concluded that only lateral twin growth may occur at higher strains.

## Work Hardening

The stress strain curves for unalloyed tungsten and the W-Re alloys were similar to those observed previously by Garfinkle (ref. 21) in ⟨001⟩ single crystals and Stephens (ref. 22) on polycrystals of these materials; that is, the curves for unalloyed tungsten were characterized by smooth yielding followed by relatively high rates of work hardening. The stress-strain curves for alloys containing 1- to 7-percent Re showed smooth yielding followed by lower rates of work hardening than measured in unalloyed tungsten. In the 25-percent-Re alloy, yielding was again smooth, except for the presence of small load drops associated with twinning near the yield stress.

Of special interest is the temperature dependence of the work-hardening rate which is shown in figure 9. Included are data for ⟨001⟩ oriented tungsten single crystals from the work of Beardmore and Hull (ref. 23). The temperature dependence of the work-hardening rate for unalloyed tungsten is very high, but that for the W-Re alloys shows almost no variation with temperature in the range shown. The rapid increase in work-

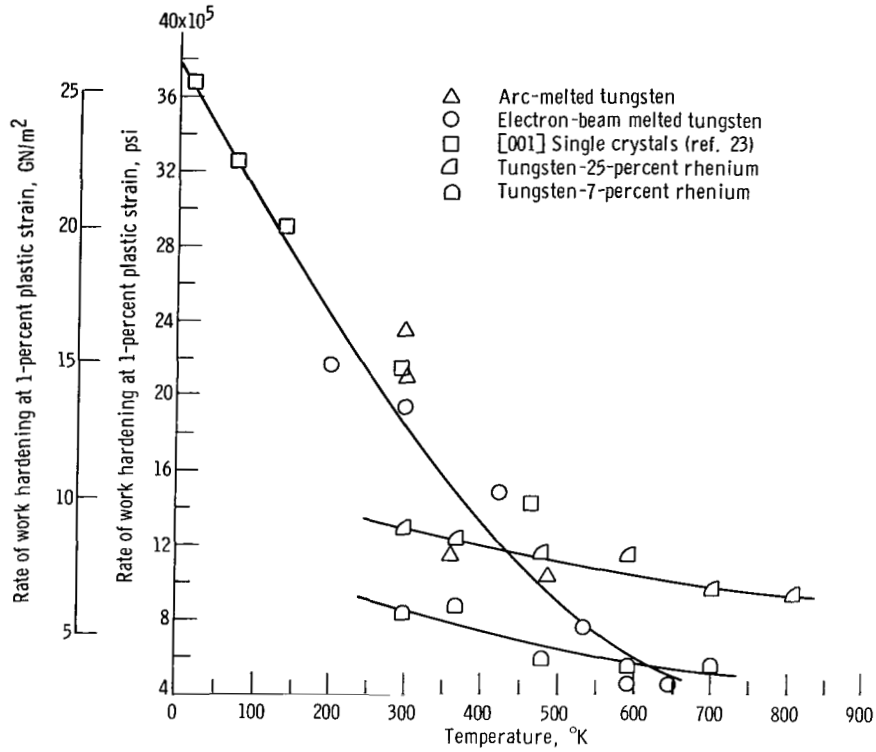


Figure 9. - Effect of temperature on rate of work hardening at 1-percent plastic strain for unalloyed tungsten and two tungsten-rhenium alloys.

hardening rate with decreasing temperature appears to be peculiar to the group VI metals, as it has also been observed in molybdenum as well (ref. 24). Other BCC metals, such as tantalum and iron, have a work-hardening rate which decreases with decreasing temperature below room temperature (ref. 25).

## Strain-Rate Sensitivity

Strain-rate cycling experiments were performed on a number of materials to determine the strain-rate sensitivity of the yield and flow stresses. In each experiment, the strain rate was cycled between the values of $8.3\times10^{-5}$ and $8.3\times10^{-4}$ $sec^{-1}$ throughout the stress-strain curve. Plots were made of the variation of the change in stress after a tenfold change in strain rate $(\Delta\sigma)_T$ against strain. The value of $(\Delta\sigma)_T$ for unalloyed tungsten was relatively independent of strain. The results for the dilute W-Re alloys were similar. For the W-25-percent-Re alloy, $(\Delta\sigma)_T$ increased with strain at low temperatures ($\leq 298^{\circ}$ K) while at higher temperatures, the variation was similar to that for unalloyed tungsten.

In order to compare the strain rate sensitivity of the yield stress on a common basis, plots, such as those just described, were made for all the tests, and the value of $(\Delta\sigma)_T$ extrapolated to zero strain was used to calculate the strain-rate sensitivity $\lambda$ as

$$\lambda = \frac{(\Delta\sigma)_T}{\Delta \ln \dot{\epsilon}} \tag{1}$$

Plots of $\lambda$ against temperature for unalloyed tungsten and the W-1-percent-Re and W-25-percent-Re alloys are shown in figure 10. The value of $\lambda$ passes through a maximum at an intermediate temperature for all the materials; this is typical of other BCC metals (ref. 26). The major differences between unalloyed tungsten and the alloys is a general decrease in $\lambda$ due to alloying and a smaller variation with temperature seen in the more concentrated alloy. This decrease in $\lambda$ is not surprising because there was a corresponding decrease in the temperature dependence of the yield stress shown in figures 6 and 7. Temperature and strain-rate dependency are thus parallel quantities.

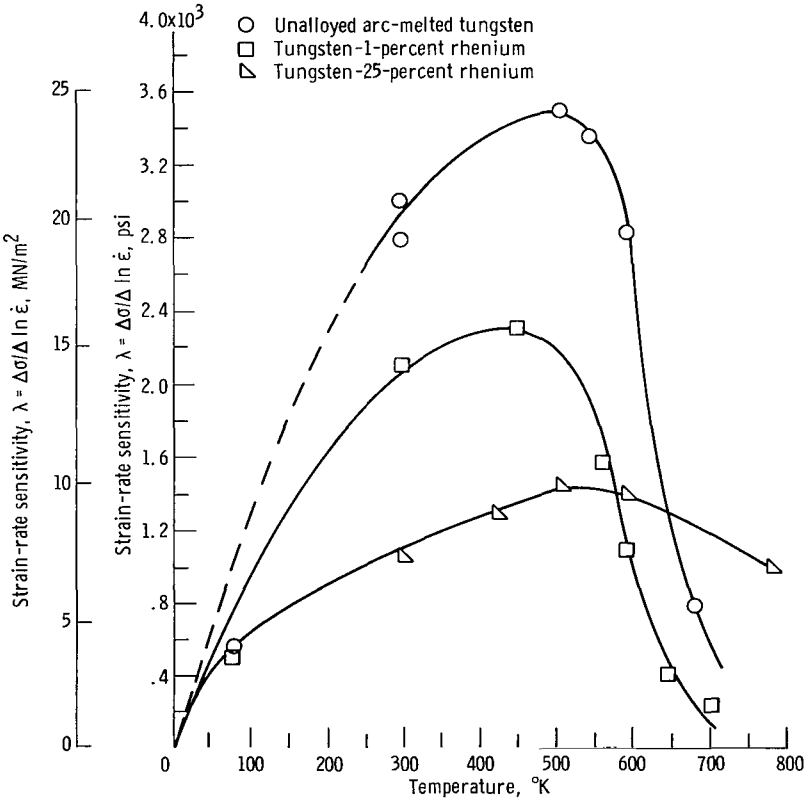


Figure 10. - Comparison of strain-rate sensitivity of unalloyed tungsten with two tungsten-rhenium alloys.

## Fractography

Metallographic studies were conducted on the fracture surfaces of most of the materials to determine the nature and origin of failure. In addition, longitudinal sections of some of the materials were examined for the presence of nonpropagating microcracks, observed previously in chromium-rhenium alloys (ref. 27).

Examination of the fracture surfaces of both unalloyed arc-melted tungsten and the dilute W-Re alloys revealed that the fractures were mainly cleavage with at most 20 percent of the fracture surface containing intergranular facets. The initiation of failure in these materials always occurred near a grain boundary, as shown in figure 11. Here, fracture apparently occurred by the intergranular parting followed by propagation of crack by cleavage. The initiation of failure can be determined by tracing the cleavage steps back to their common origin. Examination of fracture surface replicas in the electron microscope confirmed these observations.

In the W-25-percent-Re alloy, fracture was again mixed cleavage and grain boundary failure, but the percentage of the latter appeared to be increased. Gilbert, Klein, and Edington (ref. 27) have noted that in chromium-35-percent-rhenium, failure is almost totally intergranular, but cleavage failure is predominant in unalloyed chromium. The fracture origin in this alloy was more difficult to determine, but examination of longitudinal sections using the light microscope revealed the presence of twin-induced grain

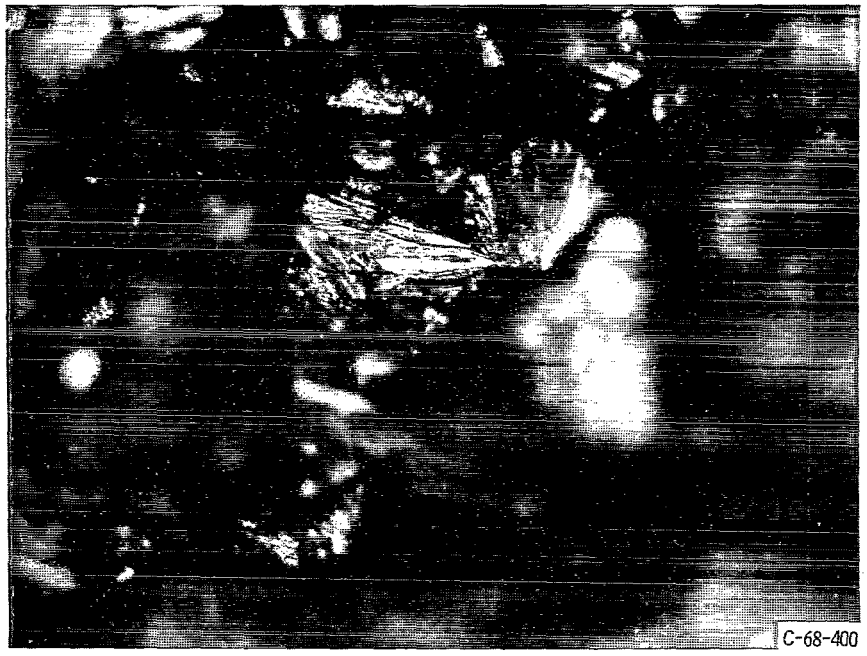


Figure 11. - Crack formed at intersection of twin and grain boundary in tungsten-25-percent rhenium tested at 298° K. X1000.

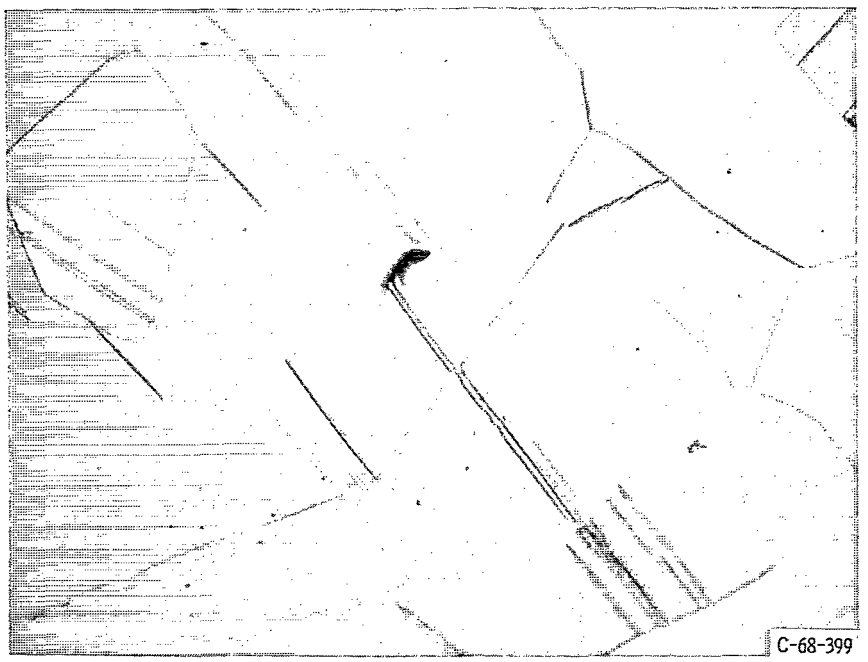


Figure 12. - Fracture surface of arc-melted tungsten fractured in tension at 298° K. X250.

boundary cracking, as illustrated in figure 12. This feature was observed throughout the gage section. It is interesting to note that this is a nonpropagating crack which indicates that the fracture behavior of this alloy has altered to the point where microcracks of less than a critical length are stable without catastrophic propagation. No microcracks were observed in unalloyed tungsten or in any of the dilute alloys, although in a few instances secondary cracks were observed branching off from the primary failure.

## DISCUSSION

In the previous sections, the temperature and strain-rate dependence of the yield and fracture properties of unalloyed tungsten and tungsten-rhenium alloys were presented. The aim of the present section is twofold. First, the data will be correlated with recent theories of yielding in the BCC metals in order to determine the effect of rhenium on dislocation mobility in tungsten. Second, the decrease in the ductile-brittle transition temperature conferred by rhenium additions will be discussed.

## Temperature and Strain Rate Dependence of Yield Stress

The object of this section is to analyze the data for the temperature and strain-rate dependence of the yield stress in order to ascertain the relevant dislocation mobility parameters. In general, the techniques of Conrad and Hayes (ref. 8) were followed in this investigation. These have been highly successful in correlating data from other BCC metals.

It is common practice to divide the yield stress into a temperature dependent (thermal component) and a temperature independent (athermal component) portion. This may be represented by

$$\sigma_y = \sigma^* + \sigma_\mu \tag{2}$$

The thermal component of the yield stress $\sigma^*$ is commonly known as the effective stress because it is this portion of the total applied stress which assists thermal fluctuations in pushing a dislocation past the various obstacles in the crystal. Such obstacles are usually classified as short range because their energy is spread out over a few interatomic spacings. The athermal component of the yield stress $\sigma_\mu$ represents the stress necessary to overcome long-range obstacles where the energy is spread over a wider distance and thermal fluctuations cannot assist the stress in bypassing them.

If only one dislocation mechanism is controlling the yield stress, then one may write a rate equation for the deformation as (ref. 26)

$$\dot{\epsilon} = \dot{\epsilon}_o \exp\left(\frac{H_o - V^*\sigma^*}{kT}\right) \tag{3}$$

where $\dot{\epsilon}$ is the applied strain rate, $\dot{\epsilon}_c$ is a frequency factor, $H_o$ is the thermal energy needed to bypass the obstacle in the absence of stress, k is Boltzmann's constant, T is temperature, and $V^*$ is the activation volume for deformation. The term $V^*\sigma^*$ represents the work performed in moving past the obstacle. The activation volume is usually stress dependent. It may be obtained from the strain-rate sensitivity as (ref. 26)

$$V^* = kT\left(\frac{\partial \ln \dot{\epsilon}}{\partial \sigma^*}\right)_T = \frac{kT}{\lambda} \tag{4}$$

where the derivative of stress in the strain-rate sensitivity is replaced by the derivative of the effective stress because this is the only portion of the stress which is strain-rate dependent. The quantity $H_o$ is obtained from a plot of the activation energy H against

stress, where H is given as $H_o - V^*\sigma^*$. The activation energy may be determined from both the temperature and strain-rate dependence of the yield stress as

$$H = -\frac{kT^2}{\lambda}\left(\frac{\partial\sigma^*}{\partial T}\right)_{\dot{\epsilon}} \tag{5}$$

Thus, measurement of $H_o$ and $V^*$ as a function of stress allows one to characterize completely the deformation processes occurring. The final step is then to compare the results with the identical quantities calculated from theory for a particular obstacle. In this section, the relevant parameters will be calculated for tungsten and the W-Re alloys.

As an initial step in the separation of the yield stress into its two components, a procedure given by Conrad and Hayes (ref. 28) will be employed. Here, the yield stress at two temperatures is compared by subtracting the yield stress at some reference temperature $T_r$ from the yield stress at the temperature of interest T:

$$\sigma_T - \sigma_{T_r} = (\sigma_T^* + \sigma_{\mu T}) - \left(\sigma_{T_r}^* + \sigma_{\mu T_r}\right) \tag{6}$$

Because the stress $\sigma_\mu$ is independent of temperature (except for the small temperature dependence of the elastic constants), we obtain

$$\sigma_T - \sigma_{T_r} = \sigma_T^* - \sigma_{T_r}^* \tag{7}$$

Thus, a plot of the stress difference in equation (6) as a function of temperature, represents the variation of the effective stress with temperature. This difference in stress is plotted in figure 13 for both unalloyed tungsten and the W-Re alloys. For convenience $T_r$ was taken as $589^\circ$ K. It is evident that rhenium decreases the thermal component of the yield stress in tungsten. At $77^\circ$ K, this reduction is from 178 000 psi (1227 $MN/m^2$) for unalloyed tungsten to 57 000 psi (393 $MN/m^2$) for the W-25-percent-Re alloy. Smaller reductions are noted for the more dilute alloys.

Although decreases in thermal component of the yield stress are evident in figure 13, reference to figure 7 indicates that the yield stresses at temperatures above approximately $400^\circ$ K increase with increasing rhenium content. This is an indication of an increase in the athermal component of the yield stress with alloying, which becomes predominant at the higher temperatures.

The strain-rate sensitivity data of figure 10 can now be employed with equation (4) to calculate the activation volume for the process. This is shown in figure 14 plotted as a function of the thermal component of the yield stress from figure 13. The activation volume is normalized by dividing by the cube of the Burgers vector (ref. 26). It can be

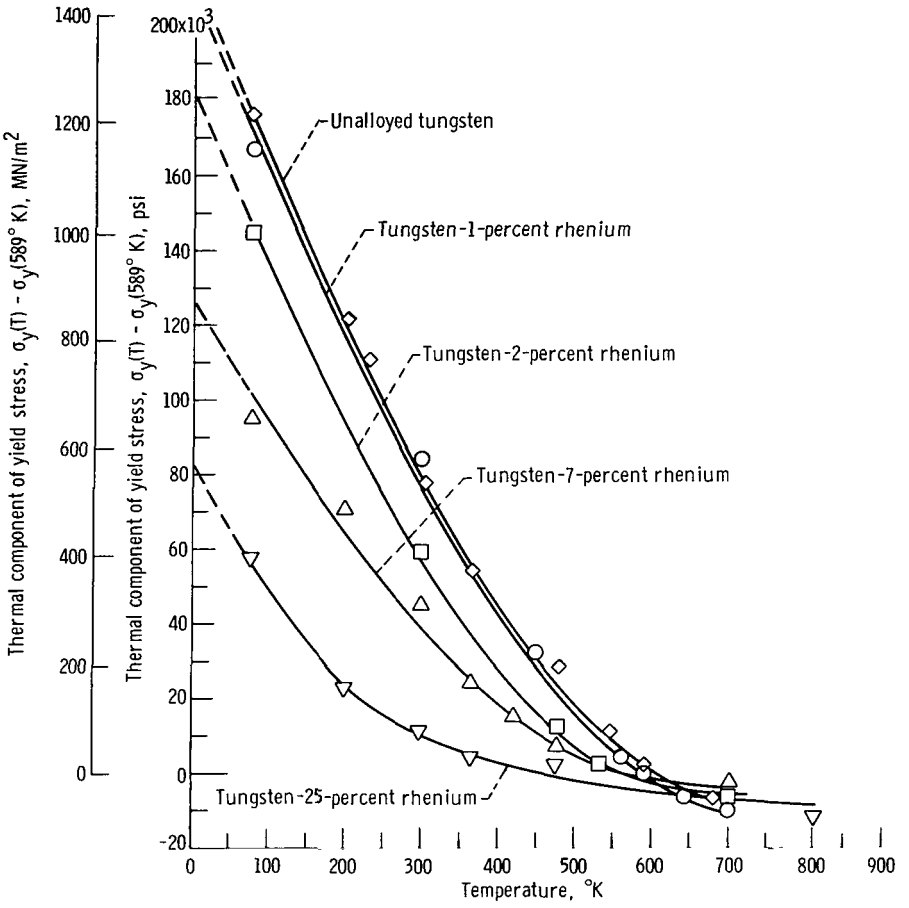


Figure 13. - Temperature dependence of thermal component of yield stress for tungsten and tungsten-rhenium alloys.

noted from figure 14 that all the data fall reasonably on the same curve, indicating that the activation volume is a single function of the effective stress in both unalloyed tungsten and the alloys. This suggests that a similar obstacle controls plastic deformation in all the materials.

The second quantity needed to characterize the deformation is $H_o$. This is most accurately determined by combined temperature and strain cycling on the same specimen to obtain values of H (eq. (5)) as a function of temperature. Extrapolation of H to the temperature where $\sigma^* = 0$ yields $H_o$. In the present study, temperature cycling studies were not conducted; however, $H_o$ may be approximated to indicate its change with composition. Equation (3) may be rewritten as follows:

$$\sigma^* V^* = H_o + kT \ln(\dot{\epsilon}_o \dot{\epsilon}) \tag{8}$$

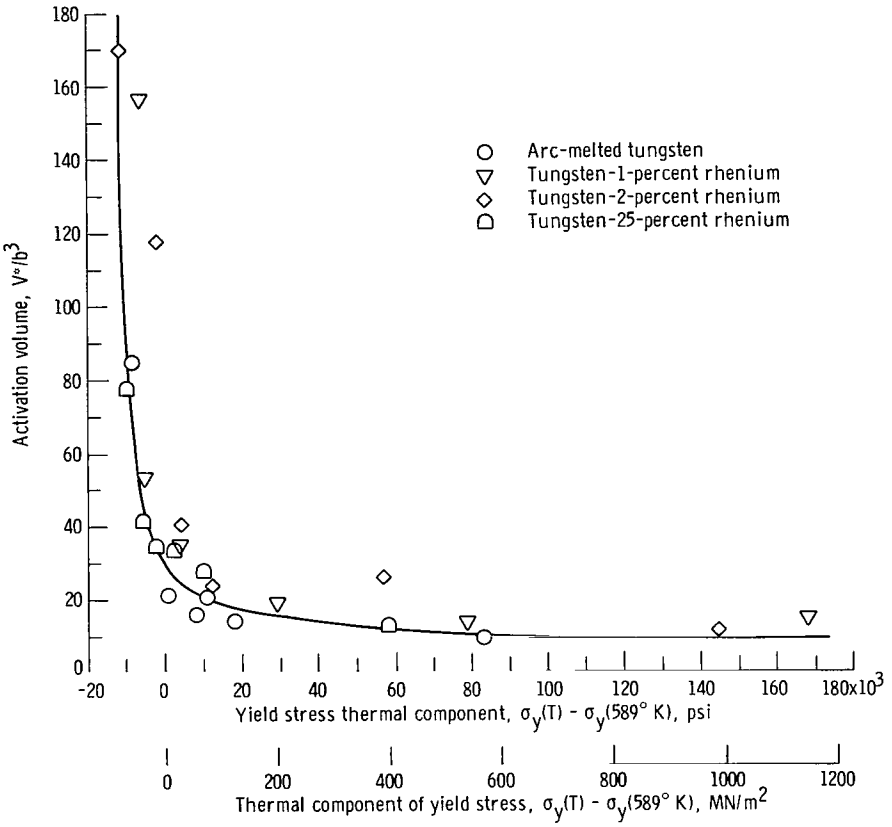


Figure 14. - Stress dependence of activation volume for all materials.

At absolute zero, the relation becomes

$$H_o = (\sigma^*)_{T=0} V^* \tag{9}$$

where $(\sigma^*)_{T=0}$ is now the effective stress at absolute zero. The change of $H_o$ with composition may be approximated by noting from figure 14 that $V^*$ is nearly independent of stress at low temperatures. Thus $H_o$ is approximately proportional to $(\sigma^*)_{T=0}$. The data in figure 13 give the variation of $\sigma_T - \sigma_{T_r}$ with temperature and composition. In the appendix a method for computing $\sigma^*$ and its extrapolation to $T = 0^o$ K are given. The values of $(\sigma^*)_{T=0}$ are listed in table V. Note that it decreases continuously with increasing rhenium content. Equation (9) then implies that $H_o$ also decreased similarly with composition. In the next section, a physical interpretation of $H_o$ is given, and additional evidence for this composition dependence is presented.

TABLE V. - PARAMETERS USED IN

DORN-RAJNAK ANALYSIS

| Rhenium composition, percent | Effective stress at absolute zero, $\sigma_o^*$ | | Temperature for $\sigma^* = 0$, $T_0$, $^oK$ |
|---|---|---|---|
| | ksi | $MN/m^2$ | |
| 0 | 228.5 | 1578 | 725 |
| 1.0 | 221.0 | 1520 | 680 |
| 2.0 | 204.0 | 1410 | 680 |
| 7.0 | 146.8 | 1010 | 700 |
| 25.0 | 96.0 | 672 | 435 |

## Dorn-Rajnak Treatment of Data

This section correlates the parameters calculated in the previous section with recent theories of yielding in the BCC metals. Although several theories of yielding have been suggested in recent years, only a few appear now to have survived a critical comparison with available experimental results. The most successful theories have been those in which the rate-controlling mechanism is one involving the intrinsic properties of the crystal lattice rather than an interaction with either impurity atoms or other dislocations. A mechanism which has gained much favor in recent years is overcoming the Peierls stress by the nucleation of kink pairs in screw dislocations (refs. 26 and 29). The Peierls stress represents an obstacle, due to the periodic variation of energy in a crystal, and arises because of the necessity of the dislocation core to change its configuration as it passes between adjacent equilibrium positions in the lattice. The double kink mechanism allows a dislocation to move by initially permitting a small segment of the line to move over the Peierls barrier. Once the nucleation of this loop is complete, the kinks (the sides of the loop) are able to move easily along the line and produce the forward motion of the entire dislocation by one slip spacing. The nucleation of kinks can occur under the combined influence of stress and temperature. The double kink mechanism of overcoming the Peierls stress has been examined in detail by Dorn and Rajnak (ref. 29) and critically applied to a number of BCC metals by Christian and Masters (ref. 25) and Guyot and Dorn (ref. 30). The Dorn-Rajnak treatment results in theoretical plots of the yield stress against temperature that may be compared with experimental data. Figure 15 shows the variation of the effective yield stress with temperature for unalloyed tungsten and the W-Re alloys. The effective stress is plotted as a ratio of the value at a given temperature to that extrapolated to absolute zero. The temperature is normalized

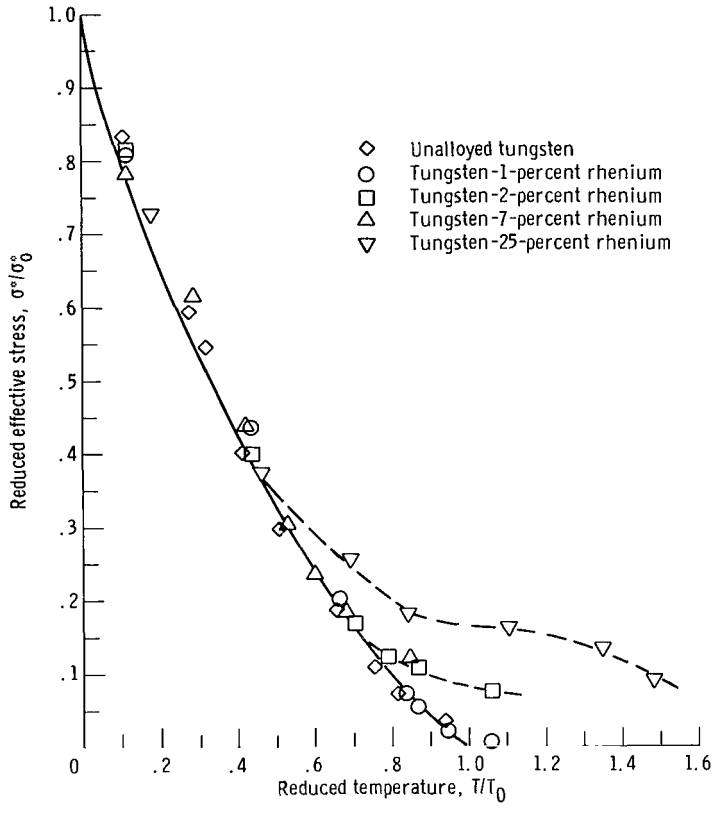


Figure 15. - Dorn-Rajnak plot for tungsten and tungsten-rhenium alloys.

by a temperature $T_0$ above which the kinks may be nucleated by thermal energy alone. The solid line is the variation required by theory, and the data were fitted by employing the extrapolated effective stresses (see appendix) and by adjusting the parameter $T_0$. The values of $T_0$ and $\sigma_o^*$ are given in table V. Dorn and Rajnak actually give three different curves of this type for different shapes of the Peierls energy barrier. I have chosen the curve for a simple parabolic barrier for convenience because the other curves only vary by about 10 percent from it.

The degree of fit with the Dorn-Rajnak plot varies between the materials. For unalloyed tungsten and W-1-percent Re, the fit is excellent over the entire temperature range. But pronounced deviations exist at higher temperatures for the other alloys. This is particularly evident in the W-25-percent-Re alloy. Here, the deviations occur above approximately $200^{\circ}$ K. This infers that a change in deformation mechanism occurs in the alloy at that temperature. Before attending to these deviations, the parameters obtained from the plot in figure 15 will be discussed. The effective stress at $0^{\circ}$ K is identified by Dorn and Rajnak as the Peierls stress $\tau_p$ (where $\tau_p$ is a shear stress). The value of $T_0$ is directly proportional to the energy to form a pair of kinks $H_o$. The values for the

parameters in table V indicate that both $T_0$ and $\sigma_o^*$ are reduced by alloying with rhenium. In the Dorn-Rajnak treatment, this infers a reduction in the Peierls stress and in the kink nucleation energy. The latter term may also be identified with the value of $H_o$ calculated in the previous section which also decreased with increasing rhenium content.

A reduction of the Peierls stress by alloying in BCC metals has been suggested previously to explain decreases in the low-temperature yield stress of tantalum-rhenium single crystals (ref. 17). Gilbert, Klein, and Edington (ref. 27) arrived at a similar conclusion with regard to some low-temperature hardness results on chromium-rhenium alloys. The Peierls stress may be reduced by either an alteration of the shape or the relative height of the Peierls energy barrier. These are essentially equivalent to saying that either the width of the dislocation core is increased or that the elastic modulus is reduced. With regard to the latter, Hay and Scala (ref. 31) have reported that an addition of 3 percent rhenium reduced the shear modulus of tungsten by approximately 18 percent. The decrease in the Peierls stress for this composition was estimated from the data in table V and found to be 16 percent, which is in excellent agreement with the modulus decrease.

A more efficient manner in which the Peierls stress may be decreased by alloying is by broadening of the dislocation core. Mitchell and Raffo (ref. 17) assumed that the Peierls stress was reduced in the immediate vicinity of the solute atom. This region is then capable of acting as a kink nucleation site. This requires only a small amount of solute, that is, 0.1 to 2 percent. Alternately, if the screw dislocations are dissociated, alloying may have the effect of lowering the stacking-fault energy and subsequently increasing the width of the dislocation. In the next section, evidence is presented which points to this process as being controlling in the W-25-percent-Re alloy. The reasons for the reduction in the Peierls stress in the dilute alloys are not clear and could be any of the three possibilities mentioned.

## Deformation of the Tungsten-25-Percent-Rhenium Alloy

The Dorn-Rajnak plot in figure 15 indicated a change in deformation mechanism at higher temperatures for the alloys, particularly W-25-percent-Re. In succeeding paragraphs, it will be shown that the new mechanism may result from a lowering of the stacking-fault energy of tungsten by rhenium alloying. This is also the basis for the prominent mechanical twinning observed in this alloy and the decrease in the Peierls stress previously mentioned.

Guyot and Dorn (ref. 30) have also observed deviations for iron-manganese and iron-molybdenum alloys similar to those seen in figure 15. They attributed these deviations

to a new deformation mechanism. This mechanism assumes that screw dislocations are dissociated in BCC metals and the resulting stacking fault must be constricted in order to move them. Mitchell, Foxall, and Hirsh (ref. 32) originally suggested this as a source of the large temperature dependence of the yield stress in BCC metals.

For example, a screw dislocation with Burgers vector a/2 ⟨111⟩ can dissociate in the following manner:

$$\frac{a}{2}\langle 111\rangle \rightarrow \frac{a}{6}\langle 111\rangle + \frac{a}{3}\langle 111\rangle \tag{11}$$

The partial dislocations lie on a {112} plane and are separated by a ribbon of stacking fault. The a/3 ⟨111⟩ dislocation can further dissociate under stress on another intersecting {112} plane into two partial dislocations of the type a/6 ⟨111⟩. The resulting total dissociation may be represented by

$$\frac{a}{2}\langle 111\rangle \rightarrow \frac{a}{6}\langle 111\rangle + \frac{a}{6}\langle 111\rangle + \frac{a}{6}\langle 111\rangle \tag{12}$$

Because dissociation results in a decrease in energy of the dislocation array, the latter dissociation produces a more stable configuration and also one which is sessile because it resides on two slip planes. In order to move this configuration, the reactions in equations (11) and (12) must be reversed and this is possible only under an applies stress. A similar sessile configuration may be produced by dissocation on {110} planes, although, in this case, the final configuration consists of stacking faults on three intersecting slip planes. Arguments such as these have been highly successful in explaining many anomalies in the choice of an observed particular slip system in BCC metals (refs. 33 and 34).

Escaig (ref. 35) has derived the relations for the yield stress, activation volume, and activation energy for the recombination of these dissociated screw dislocations. For slip on {112} planes, the yield stress takes the form (ref. 35)

$$\frac{\tau_y^*}{\mu} = \frac{1}{100\pi}\,\frac{\mu b^3}{c}\,z^{3/2}\left(\frac{1}{T}\right) \tag{13}$$

where $\tau_y^*$ is the effective yield stress in shear and z is a parameter equal to

$$z = -\left[25\,\frac{\tau_y^*}{\mu} + \ln\left(1 - \frac{25\,\tau_0^*}{\mu}\right)\right] \tag{14}$$

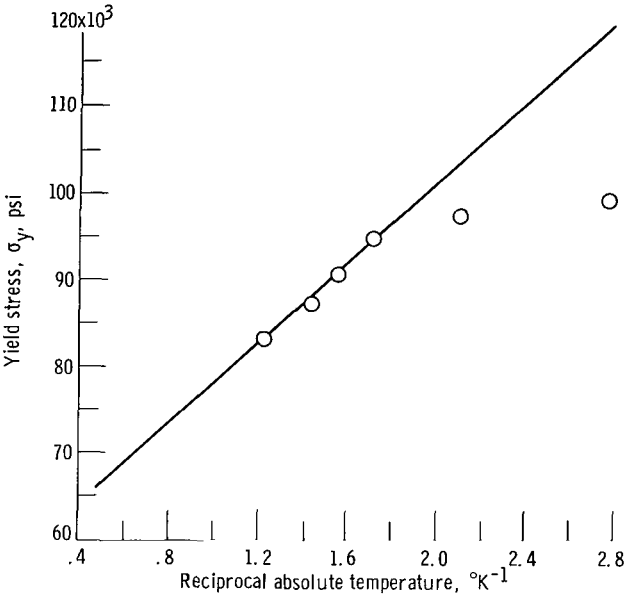


Figure 16. - Variation of yield stress with reciprocal absolute temperature for tungsten-25-percent rhenium.

where $\tau_0^*$ is the value of $\tau_y^*$ at absolute zero. This can be related to the stacking fault energy $\gamma'$ by

$$\frac{\gamma'}{\mu b} = 0.0266 - \frac{2}{3}\left(\frac{\tau_0^*}{\mu}\right) \tag{15}$$

The activation volume is given by

$$\frac{V^*}{b^3} = \frac{\mu^2}{100\pi} z^{3/2} \left(\frac{1}{\tau^*}\right)^2 \tag{16}$$

Each of these relations was tested for the W-25-percent-Re data. Figure 16 is a plot of the total yield stress against reciprocal temperature. At high temperatures, the data follow equation (13) very well. At lower temperatures, yielding occurs at a stress lower than that obtained by extrapolation of the Escaig relation. The data can be extrapolated to $1/T = 0$ to obtain a $\sigma_\mu$ value of 53 500 psi (369 $MN/m^2$). If this is subtracted from $\sigma_y$, the results for the effective stress variation can be used to obtain a stacking fault energy $\gamma'$. This was done graphically after the appropriate value of z was obtained from the slope of the straight line at high temperatures. Figure 17 shows a plot of the activation volume against $(1/\tau^*)^2$ (where $\tau^* = 1/2\ \sigma^*$) as required by equation (16).

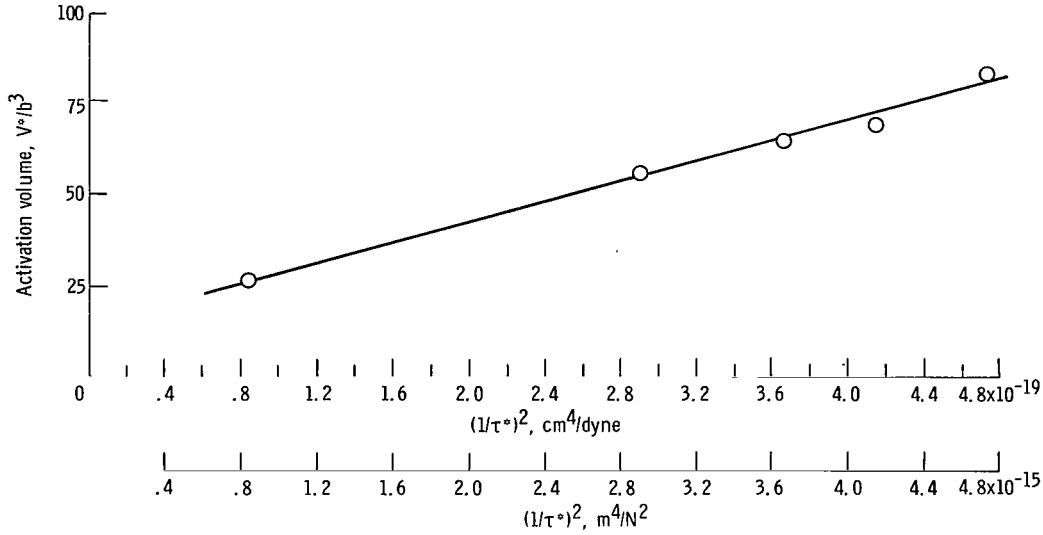


Figure 17. - Variation of activation volume with $(1/\tau^*)^2$ for tungsten-25-percent rhenium.

TABLE VI. - VALUES OF SHEAR YIELD STRESS AT ABSOLUTE ZERO AND STACKING FAULT ENERGY OBTAINED FROM ESCAIG ANALYSIS FOR SLIP ON {112} PLANES

[Normalized by shear modulus and the Burgers' vectors.]

| | $\tau_0^*/\mu$ | $\gamma'/\mu b$ | $\gamma'$, $J/cm^2$ |
|---|---|---|---|
| Yield stresses | 0.0156 | 0.0162 | $706\times10^{-7}$ |
| Activation volume | .0130 | .0180 | 785 |

Again a stacking-fault energy was obtained from the slope of the curve. The values of $\tau_0^*$ and $\gamma'$ obtained from both sets of data are given in table VI. The data are internally consistent as evidenced by the similarities of the two values obtained for $\gamma'$.

There is considerable evidence for a decrease in the stacking-fault energy by the addition of rhenium to the group VI metals. First, mechanical twinning becomes prominent at high temperatures in these alloys, indicating that the twinning stress is lowered. Simple models of the twinning stress (ref. 36) show it to be proportional to the stacking-fault energy and hence a lowering of $\gamma'$ would promote a lowering of the twinning stress. In addition, Votava (ref. 37) and Ogawa and Maddin (ref. 38) have made direct observa-

tions of stacking faults in molybdenum-35 percent rhenium by transmission electron microscopy. Ralph and Brandon (ref. 39) observed stacking faults by field ion microscopy in W-5- and W-26-percent-Re alloys. Stacking faults have not been observed in unalloyed tungsten. Aqua and Wagner (ref. 40) also noticed an increase in the fault probability in W-20-percent Re by studying the X-ray line broadening in heavily deformed samples.

In summary, the cumulative evidence presented herein implies a decreased stacking-fault energy in W-Re alloys. Because the decreased value of $\gamma'$ implies an increased dislocation width, a lower Peierls stress should result. Arsenault (ref. 41) has indicated that only a small increase in the width of the dislocation core is necessary to produce a large decrease in the Peierls stress. The calculation showed that an increase in width from b to 2b results in a reduction in the Peierls stress by a factor of 100. An additional factor which deserves mention here is that studies of slip lines in W-Re and molybdenum-rhenium alloys (refs. 21 and 27) indicate that {112} slip becomes a preferred mode. This suggests that the decrease in the stacking-fault energy may be anisotropic with a consequent lower critical resolved shear stress on {112} planes.

## Ductile-Brittle Transition

A measure of the probability of brittle fracture in a given material is the relative ease at which the energy stored near a crack tip can be dissipated. If the motion of dislocations is very difficult, the energy is released as the surface energy of the crack, and the material will be completely brittle. Hull, Beardmore, and Valentine (ref. 42) have seen indications that this is the case for unalloyed tungsten at $77^{\circ}$ K. If plastic deformation can be made to occur readily, more energy can be released in this way, which results in a blunting of the crack tip.

In order to blunt the crack, large amounts of plastic deformation should precede the moving crack. This requires a relatively high mobility of dislocations and/or a high mobile dislocation density. The decrease in the effective stress as a result of alloying with rhenium observed in this study indicates an increased value of the dislocation mobility at a given stress. In addition, Stephens (ref. 22) observed that the dislocation multiplication rate in tungsten is increased by alloying with rhenium. Thus, at a given stress and temperature, alloying with rhenium promotes an increase in the plastic-strain rate in front of a moving crack, with subsequent crack blunting. In the W-25-percent-Re alloy, this has progressed to the point where cracks below the critical size for propagation are observable in the light microscope (see fig. 10).

In contrast, no stable microcracks were observed in the dilute alloys. This suggests that crack initiation at or near grain boundaries is rate controlling as in unalloyed tung-

sten or that the critical crack length is too small to be observed.

Although we have observed a continuous decrease in the Peierls' stress with increasing rhenium content, Klopp, Witzke, and Raffo (ref. 7) observed that the transition temperature passes through a minimum at low rhenium contents. This may result from two competing factors. First, the propensity for crack blunting is increased because of the higher dislocation mobility. However, the total stress normal to the crack increases because of the presence of an increasing athermal component of the yield stress due to solid solution hardening. This balance between the tendency for crack blunting and the increased applied stress may lead to a minimum in the transition temperature. At higher rhenium contents, the effective stress has decreased to the point where it now plays a bigger role and hence the transition temperature begins to decrease again.

## CONCLUSIONS

From a study of the mechanical properties of tungsten-rhenium alloys, the following conclusions have been reached:

1. The temperature and strain rate dependence of the yield stress of tungsten is decreased by alloying with rhenium.

2. The work-hardening rate at 1-percent plastic strain for unalloyed tungsten increases rapidly with decreasing temperature, but it is relatively independent of temperature in tungsten-rhenium alloys in the temperature range $300^{\circ}$ to $800^{\circ}$ K.

3. The yielding of unalloyed tungsten and dilute tungsten-rhenium alloys is consistent with a model involving the nucleation of kink pairs over the Peierls' barrier. Alloying with rhenium reduced the Peierls' stress, presumably through a reduction in the stacking-fault energy.

4. Yielding appears to be controlled by the double kink mechanism at low temperatures in tungsten-25-percent rhenium. At high temperatures, a mechanism involving the recombination of dissociated screw dislocations fits the data better, which indicates a reduced stacking-fault energy.

5. The reduction in the transition temperature in tungsten-rhenium alloys seems to arise from an increased plastic strain at crack tips as a result of increased dislocation mobilities and multiplication rates.

Lewis Research Center,
National Aeronautics and Space Administration,
Cleveland, Ohio, January 22, 1968,
129-03-02-02-22.

# APPENDIX - DETERMINATION OF EFFECTIVE STRESS

In order to determine the value of the effective stress $\sigma^*$, the value of the athermal component $\sigma_\mu$ should be known. Consider a temperature $T_0$ where $\sigma^* = 0$. This would correspond to the temperature where thermal energy is able to push the dislocation past the obstacle without the aid of stress. At and above $T_0$, the temperature dependence of the yield stress will be that given by the temperature variation of $\sigma_\mu$. As indicated previously, the only contribution here is that due to the temperature dependence of the elastic constants. Thus, $T_0$ will be defined when

$$\frac{d\sigma_y}{dT} = \frac{dM}{dT} \tag{A1}$$

where $M$ is the elastic modulus. Plots of $d\sigma/dT$ against temperature were extrapolated to the temperature where equation (A1) was obeyed. The stress at this temperature was thus taken as the athermal component $\sigma_\mu$ which was subtracted from $\sigma_y$ to obtain $\sigma^*$. The modulus data were taken from Armstrong and Brown (ref. 43).

The extrapolation of $\sigma^*$ to absolute zero was performed in a number of ways. The most consistent results arose from a plot of $\ln \sigma^*$ against $T$. This method has been previously employed by Conrad (ref. 26).

## REFERENCES


1. Klopp, William D.; and Raffo, Peter L.; Effects of Purity and Structure on Recrystallization, Grain Growth, Ductility, Tensile, and Creep Properties of Arc-Melted Tungsten. NASA TN D-2503, 1964.

2. Seigle, L. L.; and Dickinson, C. D.; Effect of Mechanical and Structural Variables on the Ductile-Brittle Transition in Refractory Metals. Refractory Metals and Alloys II. I. Perlmutter and M. Semchyshen, eds., Interscience Publishers, 1963, p. 65.

3. Lawley, A.; Van den Sype, J.; and Maddin, R.: Tensile Properties of Zone-Refined Molybdenum in the Temperature Range 4.2 - 373° K. J. Inst. Metals, vol. 91, 1962-63, pp. 23-28.

4. Orehotsky, J. L.; and Steinitz, R.: The Effect of Zone Purification On the Transition Temperature of Polycrystalline Tungsten. Trans. AIME, vol. 224, no. 3, June 1962, pp. 556-560.

5. Hahn, G. T.; Gilbert, A.; and Jaffe, R. I.: The Effects of Solutes on the Brittle-Ductile Transition in Refractory Metals. Refractory Metals and Alloys II. I. Perlmutter and M. Semchyshen, eds., Interscience Publishers, 1963, p. 23.

6. Dickinson, J. M.; and Richardson, L. S.: The Constitution of Rhenium-Tungsten Alloys. Trans. ASM, vol. 51, 1959, pp. 758-771.

7. Klopp, William D.; Witzke, Walter R.; and Raffo, Peter L.: Mechanical Properties of Dilute Tungsten-Rhenium Alloys. NASA TN D-3483, 1966.

8. Jaffe, R. I.; Maykuth, D. J.; and Douglass, R. W.: Rhenium and The Refractory Platinum-Group Metals. Symposium on Refractory Metals and Alloys. M. Semchyshen and J. J. Harwood, eds., Interscience Publishers, 1961, pp. 383-463.

9. Klopp, W. D.; Holden, F. C.; and Jaffee, R. I.: Further Studies on Rhenium Alloying Effects in Molybdenum, Tungsten, and Chromium. Battelle Memorial Inst. (Contract NONR-1512(00)), July 12, 1960.

10. Stephens, Joseph R.; and Klopp, William D.: Ductility Mechanisms and Superplasticity in Chromium Alloys. NASA TN D-4346, 1967.

11. Raffo, Peter L.; and Klopp, William D.: Mechanical Properties of Solid-Solution and Carbide-Strengthened Arc-Melted Tungsten Alloys. NASA TN D-3248, 1966.

12. Wessel, E. T.: Refrigeration Techniques and Apparatus for Very Low Temperatures (to 4.2 K). Refrigerating Eng., vol. 65, no. 10, Oct. 1957, pp. 37-45.

13. Alers, G. A.; Armstrong, R. W.; and Bechtold, J. H.: The Plastic Flow of Molybdenum at Low Temperatures. Trans. AIME, vol. 212, no. 4, Aug. 1958, pp. 523-528.

14. Low, John R., Jr.: Microstructural Aspects of Fracture. Fracture of Solids. Vol. 20. D. C. Drucker and J. J. Gilman, eds., Interscience Publishers, 1963, pp. 197-236.

15. Wronski, A.: The Temperature-Dependence of Yield and Brittle-Fracture Stresses in Polycrystalline Molybdenum. J. Inst. Metals, vol. 92, pt. 11, July 1964, pp. 376-377.

16. Wronski, A.; and Fourdeux, A.: Slip-Induced Cleavage in Polycrystalline Tungsten. J. Less Common Metals, vol. 6, 1964, pp. 413-429.

17. Mitchell, T. E.; and Raffo, P. L.: Mechanical Properties of Some Tantalum Alloys. Can. J. Phys., vol. 45, no. 2, pt. 3, 1967, pp. 1047-1062.

18. Horne, G. T.; Roy, R. B.; and Paxton, H. W.: Tensile Properties of Single Crystals of Iron-Chromium Alloys. J. Iron Steel Inst., vol. 201, no. 2, Feb. 1963, pp. 161-167.

19. Urakami, A.; Marcus, H. L.; Meshii, M.; and Fine, M. E.: Precipitation Strengthening of Fe-6 At. % Mo. Trans. ASM, vol. 60, no. 3, Sept. 1967, pp. 344-351.

20. Underwood, Erwin E.; and Coons, William C.: The Role of Quantitative Stereology in Deformation Twinning. R. E. Reed-Hill, J. P. Hirth, and H. C. Rogers, eds., Gordon and Breach Science Publ., 1964, p. 405.

21. Garfinkle, M.: Room-Temperature Tensile Behavior of ⟨100⟩ Oriented Tungsten Single Crystals with Rhenium in Dilute Solid Solution. NASA TN D-3190, 1966.

22. Stephens, J. R.: Transmission Microscopy Study of Deformation of Tungsten and Its Alloys. Paper Presented at the Fall Meeting, AIME, Chicago, Ill., Oct. 30 - Nov. 3, 1966.

23. Beardmore, P.; and Hull, D.: Deformation and Fracture of Tungsten Single Crystals. J. Less Common Metals, vol. 9, no. 3, Sept. 1965, pp. 168-180.

24. Lawley, A.; and Gaigher, H. L.: Deformation Structures in Zone-Melted Molybdenum. Phil. Mag., vol. 10, no. 103, July 1964, pp. 15-33.

25. Christian, J. W.; and Masters, B. C.: Low-Temperature Deformation of Body-Centered Cubic Metals. Proc. Roy. Soc., ser. A, vol. 281, no. 1385, Sept. 8, 1964, pp. 223-257.

26. Conrad, H.: The Cryogenic Properties of Metals. High-Strength Materials. V. F. Zackay, ed., John Wiley & Sons, Inc., 1965, pp. 436-509.

27. Gilbert, A.; Klein, M. J.; and Edington, J. W.: Investigation of Mechanical Properties of Chromium, Chromium-Rhenium, and Derived Alloys. Battelle Memorial Inst. (NASA CR-81225), Aug. 31, 1966.

28. Conrad, H.; and Hayes, W.: Correlation of the Thermal Component of the Yield Stress of the BCC Metals. Trans. ASM, vol. 56, no. 1, Mar. 1963, pp. 125-134.

29. Dorn, John E.; and Rajnak, Stanley: Nucleation of Kink Pairs and the Peierls Mechanism of Plastic Deformation. Trans. AIME, vol. 230, no. 5, Aug. 1964, pp. 1052-1064.

30. Guyot, Pierre; and Dorn, John E.: A Critical Review of the Peierls Mechanism. Can. J. Phys., vol. 45, no. 2, pt. 3, 1967, pp. 983-1016.

31. Hay, D. R.; and Scala, E.: Effect of Carbon Addition on the Shear Modulus of Tungsten and a Tungsten . 3% Rhenium Alloy. Paper presented at the Fall Meeting, AIME, Chicago, Ill. Oct. 30-Nov. 3, 1966.

32. Mitchell, T. E.; Foxall, R. A.; and Hirsch, P. B.: Work-Hardening in Niobium Single Crystals. Phil. Mag., vol. 8, 1963, pp. 1895-1920.

33. Bowen, K. D.; Christian, J. W.; and Taylor, G.: Deformation Properties of Niobium Single Crystals. Can. J. Phys., vol. 45, no. 2, pt. 3, 1967, pp. 903-938.

34. Foxall, R. A.; Duesbery, M. S.; and Hirsch, P. B.: The Deformation of Niobium Single Crystals. Can. J. Phys., vol. 45, no. 2, pt. 2, 1967, pp. 607-630.

35. Escaig, B.: Origin of the Elastic Limit of BCC Metals at Low Temperature. J. Physique, vol. 28, no. 2, Feb. 1967, pp. 171-186.

36. Venables, J. A.: Deformation Twinning in FCC Metals. Deformation Twinning. R. E. Reed-Hill, J. P. Hirth, and H. C. Rogers, eds., Gordon and Breach Science Publ., 1964, p. 77.

37. Votava, E.: Polygonization and Stacking Faults in Molybdenum-Rhenium Alloys. Acta Met., vol. 10, no. 8, Aug. 1962, pp. 745-747.

38. Ogawa, K.; and Maddin, R.: Direct Observations of Dislocations in Molybdenum and Molybdenum-Rhenium Alloys. J. Phys. Soc. Japan, vol. 18, Supple. I, 1963, pp. 81-87.

39. Ralph, Brian; and Brandon, D. G : A Field Ion Microscope Study of Some Tungsten-Rhenium Alloys. Phil. Mag., vol. 8, 1963, pp. 919-934.

40. Aqua, E. N.; and Wagner, C. N. J.: Faulting in Cold Worked Ta-10% Re and W-20% Re. Trans. ASM, vol. 59, no. 3, Sept. 1966, pp. 367-373.

41. Arsenault, R. J.: The Double-Kink Model of Low-Temperature Deformation of BCC Metals and Solid Solutions. Acta Met. vol. 15, no. 3, Mar. 1967, pp. 501-511.

42. Hull, D.; Beardmore, P.; and Valentine, A. P.: Crack Propagation in Single Crystals of Tungsten. Phil. Mag., vol. 12, 1965, pp. 1021-1041.

43. Armstrong, Philip E.; and Brown, Harry L.: Dynamic Young's Modulus Measurements Above 1000° C on Some Pure Polycrystalline Metals and Commercial Graphites. Trans. AIME, vol. 230, no. 5, Aug. 1964, pp. 962-966.



NASA-Langley, 1968 — 17 E-4158

*"The aeronautical and space activities of the United States shall be conducted so as to contribute . . . to the expansion of human knowledge of phenomena in the atmosphere and space. The Administration shall provide for the widest practicable and appropriate dissemination of information concerning its activities and the results thereof."*

—NATIONAL AERONAUTICS AND SPACE ACT OF 1958

# NASA SCIENTIFIC AND TECHNICAL PUBLICATIONS

TECHNICAL REPORTS: Scientific and technical information considered important, complete, and a lasting contribution to existing knowledge.

TECHNICAL NOTES: Information less broad in scope but nevertheless of importance as a contribution to existing knowledge.

TECHNICAL MEMORANDUMS: Information receiving limited distribution because of preliminary data, security classification, or other reasons.

CONTRACTOR REPORTS: Scientific and technical information generated under a NASA contract or grant and considered an important contribution to existing knowledge.

TECHNICAL TRANSLATIONS: Information published in a foreign language considered to merit NASA distribution in English.

SPECIAL PUBLICATIONS: Information derived from or of value to NASA activities. Publications include conference proceedings, monographs, data compilations, handbooks, sourcebooks, and special bibliographies.

TECHNOLOGY UTILIZATION PUBLICATIONS: Information on technology used by NASA that may be of particular interest in commercial and other non-aerospace applications. Publications include Tech Briefs, Technology Utilization Reports and Notes, and Technology Surveys.

*Details on the availability of these publications may be obtained from:*

**SCIENTIFIC AND TECHNICAL INFORMATION DIVISION**

**NATIONAL AERONAUTICS AND SPACE ADMINISTRATION**

**Washington, D.C. 20546**